

Original Research

Selenium Protects Against Cadmium-Induced Hepatotoxicity via Regulation of Lipid Metabolism and Inflammatory Pathways

Zilong Wu^{1,2,3,†}, Xinyi Chen^{1,†,§}, Xiaoying Pan^{1,2,3}, Kai Luo^{2,3}, Zixiong Zhang^{1,3},
Changyu Zhou^{1,3}, Haibo Wang^{2,3,*}, Chuying Huang^{1,3,4,*}¹Hubei Key Laboratory for Translational Research in Traditional Chinese Medicine, The Central Hospital of Enshi Tujia and Miao Autonomous Prefecture, Hubei Minzu University, 445000 Enshi, Hubei, China²College of Biological and Food Engineering, Hubei Minzu University, 445000 Enshi, Hubei, China³Hubei Provincial Key Lab of Selenium Resources and Bioapplications, 445000 Enshi, Hubei, China⁴Department of Oncology, The Central Hospital of Enshi Tujia and Miao Autonomous Prefecture, 445000 Enshi, Hubei, China*Correspondence: wanghaibo0519@126.com (Haibo Wang); huangchuying2008@126.com (Chuying Huang)

†These authors contributed equally.

§Current address: School of Public Health, Xiamen University, 361100 Xiamen, Fujian, China.

Academic Editors: Marek Kieliszek and Graham Pawelec

Submitted: 5 October 2025 Revised: 22 January 2026 Accepted: 9 February 2026 Published: 17 March 2026

Abstract

Background: Cadmium (Cd), a widespread environmental pollutant, poses significant risks to human health due to its high bioaccumulation potential and prolonged biological half-life. Selenium (Se) has been reported to exert protective effects against Cd-induced organ toxicity; however, the underlying molecular mechanisms, particularly those associated with lipid metabolism and inflammatory regulation, remain insufficiently elucidated. **Methods:** The hepatoprotective effects of Se, administered as selenomethionine (SeMet) and Se-enriched *Cardamine ensiensis* extract (CE), were investigated against Cd-induced hepatic injury using both *in vitro* (L-02 hepatocytes) and *in vivo* (C57BL/6J mice) models. **Results:** SeMet significantly attenuated Cd-induced cytotoxicity, lipid accumulation, and metabolic dysregulation in L-02 cells. In Cd-exposed mice, treatment with SeMet or CE significantly mitigated hepatic injury, steatosis, and inflammation, as evidenced by normalized serum alanine aminotransferase (ALT), aspartate aminotransferase (AST), triglyceride (TG), and total cholesterol (TC) levels, improved hepatic histoarchitecture, and reduced lipid droplet deposition. Integrated lipidomic and transcriptomic analyses demonstrated that Se supplementation restored Cd-perturbed polyunsaturated fatty acid metabolism, down-regulated lipogenic genes (*SCD1*, *Pparγ*, *Fasn*), and suppressed pro-inflammatory mediators (*Cxcl2*, *Ccl2*). **Conclusion:** Se confers hepatoprotection against Cd toxicity not only through its classical antioxidant activity but also through coordinated modulation of lipid metabolic pathways and inflammatory signaling. This study provides mechanistic insights into Se-mediated defense against Cd-induced hepatotoxicity and highlights the therapeutic potential of Se-enriched phytochemicals for mitigating the adverse effects of environmental Cd exposure.

Keywords: cadmium; selenium; chemical and drug induced liver injury; lipid metabolism; inflammation

1. Introduction

Cadmium (Cd), a widespread and bioaccumulative environmental toxicant, poses severe threats to human health owing to its prolonged biological half-life and inefficient metabolic clearance [1]. The liver and kidneys, as primary sites of xenobiotic metabolism, are particularly vulnerable to both acute and chronic Cd exposure, making them major targets of Cd-induced toxicity [2–4]. Extensive evidence indicates that Cd exerts multi-organ toxicity through diverse mechanisms, including oxidative stress, DNA damage, endoplasmic reticulum stress (ERS), apoptosis, autophagy, and reproductive system disorders [5,6]. Among these, oxidative stress and inflammation are considered key pathogenic events in Cd-mediated tissue injury, despite Cd lacking redox activity as a non-Fenton metal [7,8]. Although significant advances have been made in delineating the molecular basis of Cd toxicity, effective therapeutic

strategies to counteract its deleterious effects remain scarce. Therefore, elucidation of the molecular mechanisms underlying Cd-induced hepatic and renal injury and the development of targeted interventions represent critical research imperatives.

Selenium (Se), an essential micronutrient, is vital for maintaining human health due to its key roles in antioxidative defense, anti-inflammatory regulation, and immune modulation [9–12]. Accumulating evidence supports the protective effects of Se against Cd toxicity, with exogenous Se supplementation reported to attenuate Cd-induced cellular and tissue damage through multiple mechanisms [13]. One of the primary protective pathways involves the formation of Se–Cd complexes, which promote Cd detoxification and excretion from the body [14–16]. Furthermore, Se mitigates Cd-induced oxidative stress and ERS in renal tissues, as well as oxidative damage and programmed necrosis in the liver [17]. Se exerts its antioxidant and



anti-inflammatory functions through incorporation into selenoproteins, including glutathione peroxidase (GPx) and thioredoxin reductase (TrxR), which collectively maintain redox homeostasis and suppress inflammatory signaling cascades [18,19]. Moreover, Se has been reported to attenuate Cd toxicity through activation of the nuclear factor erythroid 2-related factor 2 (Nrf2) signaling pathway [20]. Recent studies have demonstrated that various forms of Se, including sodium selenite, selenomethionine (SeMet), nano-Se, and Se derived from *Cardamine hupingshanensis*, effectively alleviate Cd-induced toxicity in multiple organs such as the liver, kidneys, spleen, brain, and heart in both *in vivo* and *in vitro* models [20,21]. Despite these advances, the precise molecular mechanisms underlying the protective actions of Se, particularly its modulation of lipid metabolic pathways and suppression of inflammatory processes in Cd-induced hepatotoxicity, remain insufficiently elucidated.

The significance of this study is derived from the considerable public health burden associated with environmental cadmium exposure, for which no pharmacological intervention with an established safety and efficacy profile is currently available. Clinical management remains largely dependent on chelation therapy, which is frequently limited by off-target toxicity and organ-related adverse effects. This situation emphasizes the need to identify safe and effective alternative strategies and to advance beyond the conventional antioxidant framework toward a precise characterization of the molecular pathways responsible for selenium-mediated protection. Based on previous observations [21,22], the aim of this study is to elucidate the molecular mechanisms by which selenium, particularly in the form of a *Cardamine ensheensis*-derived extract enriched in SeCys₂ (CE), protects against cadmium-induced hepatotoxicity, using integrated lipidomic and transcriptomic analyses to define its regulatory effects on polyunsaturated fatty acid metabolism, lipogenic gene networks, and inflammatory signaling pathways.

2. Materials and Methods

2.1 Cell Culture

The L-02 hepatocyte line (kindly provided by Prof. Jiangfeng Wu, China Three Gorges University) was cultured in DMEM/F-12 (Gibco, 11320082, Grand Island, CA, USA) supplemented with 10% fetal bovine serum (FBS; Vivalcell, C04001-050X10, Shanghai, China) and 1% penicillin/streptomycin (Gibco, 15140-122, Grand Island, CA, USA). Cells were maintained at 37 °C in a humidified incubator containing 5% CO₂. The L-02 cells used in our laboratory have undergone recent STR profiling authentication, and the validation report has been uploaded as an attachment. Additionally, PCR testing confirmed the absence of mycoplasma contamination. As detailed in Section 2.1, the forward and reverse primer sequences employed for PCR-based mycoplasma identification in this

study were 5'-GGGAGCAAACAGGATTAGATACCCT-3' and 5'-TGCACCATCTGTCACTCTGTGTTAACCTC-3', respectively.

2.2 Cell Viability Assay

L-02 cells were seeded in 96-well plates at a density of 1×10^4 cells per well and cultured until reaching 60–70% confluency. To assess single-agent cytotoxicity, cells were treated with increasing concentrations of SeMet (0–100 μM; TargetMol, T1658, Boston, MA, USA) or CdCl₂ (0–200 μM; Macklin, C805625, Shanghai, China) for 24 hours (h). For combination studies, cells were pretreated with SeMet for 24 h, followed by 24 h exposure to CdCl₂. Cell viability was measured using the Cell Quanti-Blue assay kit (BioAssay Systems, CQBL-05K, Grand Island, CA, USA), and absorbance was recorded at 570 nm and 600 nm after a 3 h incubation with the detection reagent. The protocol was followed in accordance with the manufacturer's guidelines.

2.3 Observation of Cellular Growth Morphology

L-02 cells were plated in 6-well plates at 2×10^5 cells per well in 2 mL of culture medium. Cells were divided into four treatment groups: control (serum-free medium), Se (0.1 μM SeMet), Cd (40 μM CdCl₂), and Se+Cd (0.1 μM SeMet + 40 μM CdCl₂). Once cells reached 60–70% confluency, Se and Se+Cd groups were pretreated with SeMet for 24 h. Following, Cd and Se+Cd groups were exposed to CdCl₂ for another 24 h. After treatment, the medium was removed, and the cells were washed twice with phosphate-buffered saline (PBS). Cells were then fixed with 500 μL of 4% paraformaldehyde per well for 15 minutes, washed twice with PBS, and stained with 500 μL of crystal violet for 10 minutes in the dark. Following two further PBS washes, cell morphology was assessed via microscopic imaging.

2.4 Animal Model and Experimental Design

C57BL/6J mice (sourced from Hua Lian Ke, Wuhan, China) were housed under standardized conditions at the Central Hospital of Enshi Tujia and Miao Autonomous Prefecture, with temperature maintained at 20–26 °C, relative humidity at 40–70%, chamber pressure at 20–50 Pa, and a 12 h/12 h light-dark cycle. Animals had ad libitum access to food and water. All experimental procedures were approved by the Institutional Animal Ethics Committee (Approval No.: 202101001). A chronic Cd exposure model was established by intraperitoneal injections of CdCl₂ (2 mg/kg) [21,23] every 48 h for 4 weeks. Se supplementation was administered weekly *via* oral gavage at 7.5 μg per 20 g body weight, a dose extrapolated from human pharmacokinetics based on a maximum tolerable intake of 400 μg/day [24]. Mice were randomly assigned to six groups (n = 10 per group) [21,25]: Control (vehicle), Se (SeMet only), CE (Se-rich CE extract only), Cd (CdCl₂ only), Se+Cd (SeMet

plus CdCl₂), and CE+Cd (CE extract plus CdCl₂). One week before Cd exposure, Se and Se+Cd groups received a single SeMet pretreatment, while CE and CE+Cd groups were pretreated with CE extract to prime Se-dependent biochemical pathways. Dosing volumes were adjusted every 4 days according to body weight.

Throughout the study, mice were closely monitored for behavioral indicators (locomotor activity, fur condition), physiological parameters (food and water intake, body weight), and general clinical signs.

2.5 Sample Collection and Processing

Mice were anesthetized via intraperitoneal injection of 1.25% tribromoethanol (0.4 mL/10 g body weight). Adequate anesthesia was confirmed by the absence of a withdrawal reflex upon hind paw pinching. The animals were then euthanized by cervical dislocation, and death was verified by complete cessation of respiration and heartbeat, along with pupil dilation. Following euthanasia, blood was collected by cardiac puncture into heparinized tubes. Serum was obtained by centrifugation at 2000 ×g for 15 min at 4 °C and stored at –20 °C. Tissues were rinsed with ice-cold saline, blotted dry, and weighed. Serum samples were analyzed using an automated biochemical analyzer to measure alanine aminotransferase (ALT), aspartate aminotransferase (AST), albumin (ALB), globulin (GLO), total protein (TP), total cholesterol (TC), and triglycerides (TG) [26].

2.6 Se Quantification

The selenium content of the Cardamine extract was quantified by inductively coupled plasma–mass spectrometry (ICP–MS; Thermo Fisher Scientific, iCAP TQe, Serial No. ICAPTQe00081, Waltham, MA, USA). Calibration curves were generated using a series of working standard solutions prepared by serial dilution of a multi-element standard stock solution with ultrapure water. An internal standard solution was continuously introduced online into all calibration standards and sample solutions to correct for instrumental drift and matrix effects. Before analysis, Cardamine extract samples were sequentially diluted with ultrapure water (100-fold and 1000-fold) and analyzed directly under the same instrumental conditions.

2.7 Quantitative Real-Time PCR (qPCR) Analysis

Total RNA was extracted from liver tissues using the EASYspin Tissue & Cell RNA Kit (Aidlab, RN07, Beijing, China) following the manufacturer's protocol. RNA concentration and purity were evaluated spectrophotometrically. One microgram of total RNA was reverse-transcribed into first-strand cDNA using ToloScript All-in-One RT EasyMix for qPCR (TOLOBIO, 22107, Shanghai, China). qPCR was performed in triplicate on a CFX96 Touch Real-Time PCR Detection System using 2×Q3 SYBR qPCR Master Mix (TOLOBIO, 22204, Shanghai, China). Each 20 μL reaction contained 10 μL SYBR Green Master Mix,

0.8 μL each of forward and reverse primers (10 μM), 2 μL cDNA template, and 6.4 μL nuclease-free water. Thermal cycling was conducted with an initial denaturation at 95 °C for 30 s, followed by 40 cycles of 95 °C for 5 s and 60 °C for 30 s. Relative gene expression levels were normalized to the housekeeping gene *Gapdh* and calculated using the 2^{–ΔΔCt} method.

2.8 Statistical Analysis

All data are expressed as mean ± Standard Error of the Mean (SEM) and analyzed using GraphPad Prism 9 (GraphPad Software, Boston, MA, USA). Statistical differences among groups were evaluated using one-way analysis of variance (ANOVA), followed by Tukey's post hoc test for multiple comparisons.

3. Results

3.1 Se Mitigates Cd-Induced Hepatotoxicity by Restoring Lipid and Metabolic Balance

To investigate the protective role of SeMet against Cd-induced cytotoxicity in L-02 cells, the IC₅₀ of CdCl₂ was first determined to be 139.1 μM (Fig. 1a), while 0.1 μM was identified as the non-toxic concentration of SeMet (Fig. 1b). SeMet treatment significantly reduced Cd-induced cytotoxicity in a dose-dependent manner, with stronger protection observed at higher Cd concentrations (Fig. 1c,d). Furthermore, SeMet ameliorated Cd-induced metabolic dysregulation, as reflected by decreased levels of hepatic injury markers (AST and ALT) and lipid metabolites (TG and TC) (Fig. 1e–h). Treatment with 0.1 μM SeMet also significantly reduced lipid accumulation in L-02 cells exposed to 140 μM CdCl₂ (Fig. 1i,j).

3.2 Se Supplementation Protects Against Cd-Induced Liver Injury and Steatosis in Mice

To investigate the hepatoprotective effects of Se against Cd-induced toxicity, selenomethionine (SeMet) and Se-enriched Cardamine extract (CE) were administered in a mouse model. Cd exposure caused significant hepatic injury, characterized by a rough liver surface and firm texture, which were significantly alleviated by Se supplementation (Fig. 2a,b). Histopathological assessment using H&E staining revealed that Se supplementation significantly reduced Cd-induced hepatocellular ballooning and inflammatory cell infiltration, while Oil Red O staining demonstrated a significant attenuation of hepatic lipid accumulation (Fig. 2c,d). Serum biochemical analyses showed that Cd exposure significantly elevated the activities of liver injury markers (ALT, AST, and the AST/ALT ratio) [27,28] whereas Se supplementation restored these parameters to near-normal levels (Fig. 2e–g). In comparison, markers of hepatic synthetic function (ALB, GLO, and TP) showed no significant changes across the experimental groups (Fig. 2h–j). Moreover, Cd exposure disrupted hepatic lipid metabolism, as indicated by increased TC and TG

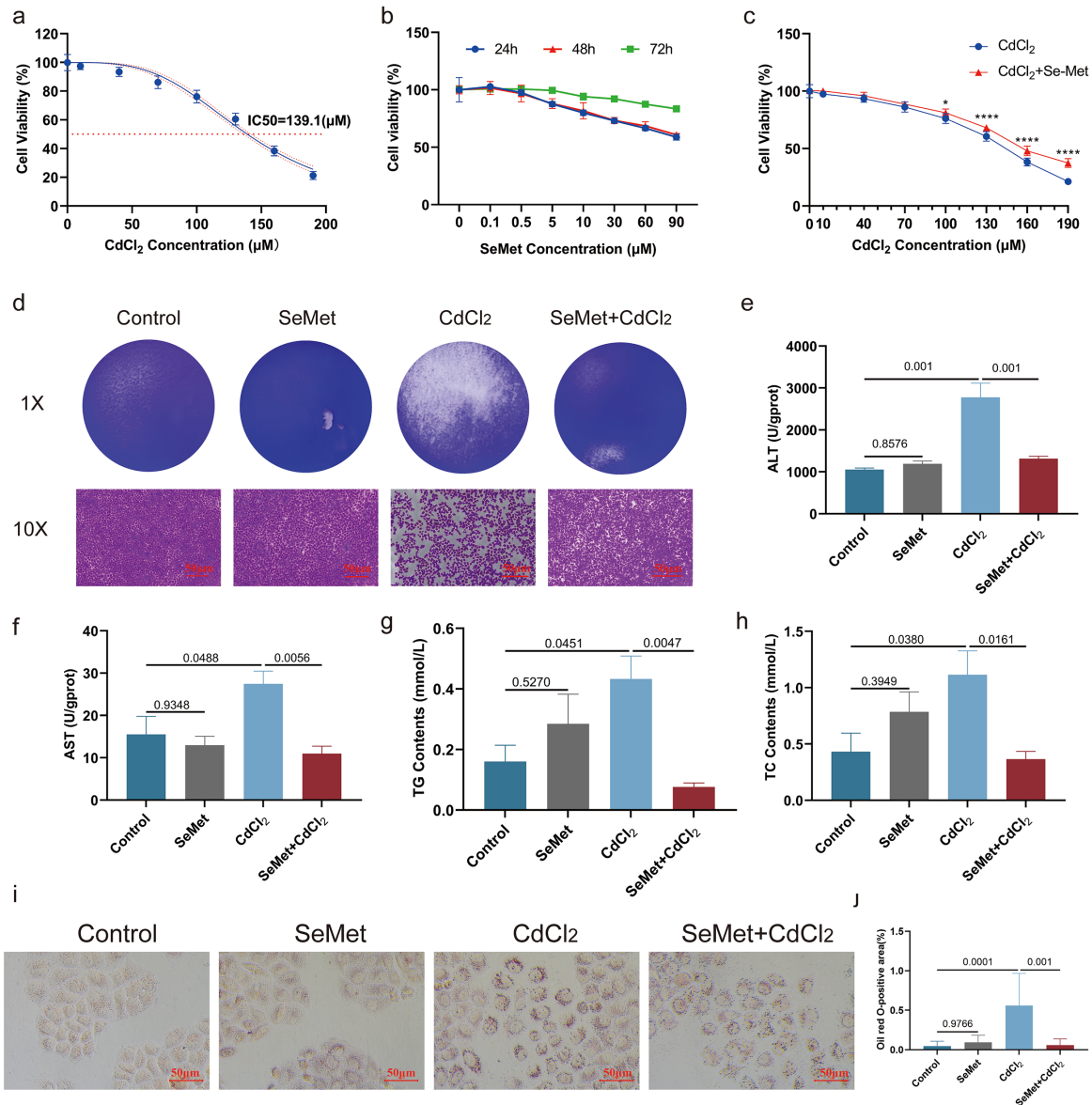


Fig. 1. Protective effects of SeMet against Cd-induced toxicity in L-02 cells. (a) Cytotoxicity of CdCl₂ in L-02 cells following 24-hour exposure. The half-maximal inhibitory concentration (IC₅₀) was determined to be 139.1 μM. (b) Assessment of L-02 cell viability after 24-hour treatment with increasing concentrations of SeMet (0–100 μM). A concentration of 0.1 μM was identified as non-cytotoxic. (c,d) Concentration-dependent cytoprotective effect of SeMet (0.1 μM) against varying CdCl₂ doses (0–190 μM). Cell viability was measured after 24-hour co-treatment. SeMet pre-treatment significantly mitigated Cd-induced cytotoxicity, with stronger protection observed at higher CdCl₂ concentrations (**p* < 0.05, *****p* < 0.0001). Scale bar in (d) = 50 μm. (e–h) Biochemical analysis showing that 24-hour pretreatment with 0.1 μM SeMet significantly reversed the elevations induced by 140 μM CdCl₂ (24 h) in: (e) ALT, (f) AST, (g) TG, and (h) TC. (i,j) Representative micrographs (i) and quantitative analysis (j) of Oil Red O staining. SeMet pretreatment (0.1 μM) significantly reduced intracellular lipid accumulation induced by 140 μM CdCl₂. Scale bar in (i) = 50 μm. Data are expressed as mean ± SEM from three independent experiments (n = 3). SeMet, Selenomethionine; Cd, Cadmium; CdCl₂, Cadmium Chloride; ALT, Alanine aminotransferase; AST, Aspartate aminotransferase; TG, Triglycerides; TC, Total cholesterol.

levels, both of which were significantly reduced following Se supplementation (Fig. 2k,l). These findings indicate that Se supplementation mitigates Cd-induced hepatotoxicity by preserving liver architecture and alleviating lipid accumulation.

3.3 Se Counteracts Cd-Induced Hepatotoxicity by Modulating Lipid Homeostasis and Inhibiting Inflammatory Responses

To elucidate the molecular mechanisms underlying the protective effects of Se against Cd-induced hepatotoxicity, a comprehensive analysis of hepatic lipid metabolism

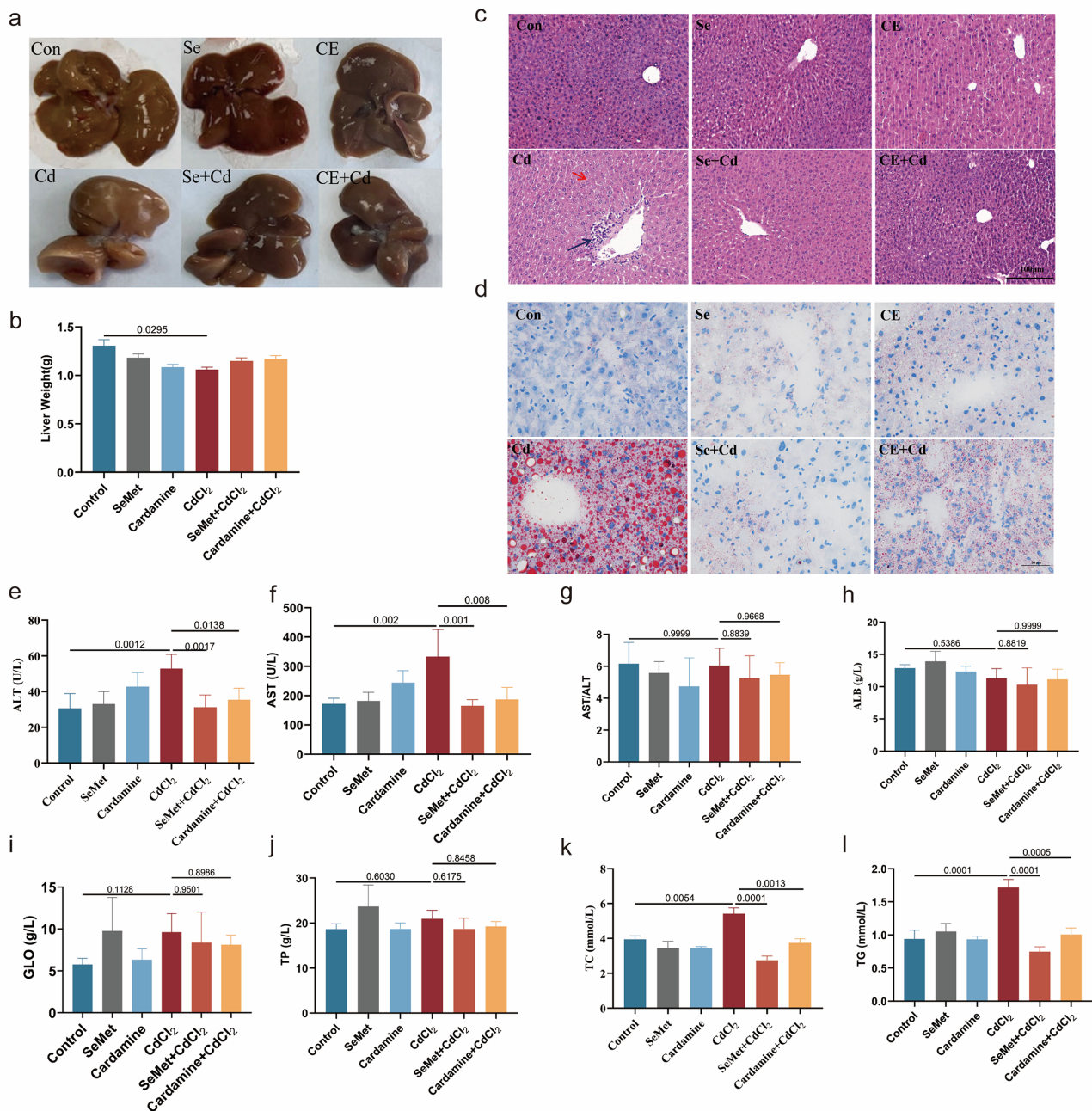


Fig. 2. Protective effects of SeMet and CE against Cd-induced hepatotoxicity in mice. Macroscopic images of livers from six experimental groups, Control (1× PBS), Se (SeMet alone), CE (CE extract alone), Cd (CdCl₂ alone), Se+Cd (SeMet+CdCl₂), and CE+Cd (CE extract+CdCl₂), revealed that Cd exposure caused visible alterations, including a rough surface and hardened texture, which were improved by both SeMet and CE supplementation (a). Liver weight in mice (b). H&E staining of liver sections showed that Cd induced hepatocyte ballooning (arrowheads) and inflammatory cell infiltration (arrows), which were significantly reduced in the Se+Cd and CE+Cd groups (c, scale bar: 100 μm). Red arrow: Liver cells damaged following cadmium exposure, exhibiting features such as cytoplasmic vacuolisation and vacuolar degeneration. Blue arrow: Inflammatory cell infiltration in the liver, primarily involving lymphocytes, macrophages and other inflammatory cells aggregated around blood vessels. Oil Red O staining demonstrated that Cd exposure led to significant microvesicular steatosis (red droplets), which was substantially attenuated by SeMet and CE co-treatment, as confirmed by quantitative analysis (d, scale bar: 50 μm). Serum levels of liver injury markers, ALT (e), AST (f), and AST/ALT ratio (g), were elevated by Cd exposure and normalized by Se supplementation. Serum markers of hepatic synthesis function, ALB (h), GLO (i), and TP (j), showed no significant differences among groups. Cd-induced dyslipidemia, reflected by increased TC (k) and TG (l), was effectively reversed by both SeMet and CE supplementation. Data are presented as mean ± SEM, (n = 6–10). CE, Cardamine extract; PBS, Phosphate-buffered saline; Se, Selenium; ALB, albumin; GLO, globulin; TP, total protein.

Table 1. The levels of main metabolites.

Accession	LCd_Mean	LCE_Cd_Mean	FC	FDR
PE(18:0p_22:5)	17450872.6	15183624.29	1.15	0.969985079
PC(18:1_14:0)	39435557.59	32130622.06	1.23	0.969985079
PC(36:1e)	302313163	179843370.8	1.68	0.887144456
PC(44:4e)	4882880.47	3840599.59	1.27	0.887144456
PC(45:2)	307264.63	430622.29	0.71	0.969985079
TG(6:0_14:3_18:2)	490932.45	363589.98	1.35	0.969985079
TG(11:0_12:2_18:2)	13452059.04	9598922.68	1.4	0.887144456
TG(12:0e_6:0_22:6)	365343327.4	280980887	1.3	0.969985079
Cer(d18:0_24:1)	8623679.74	7392526.2	1.17	0.969985079
BisMePA(40:7e)	17450872.6	15183624.29	1.15	0.969985079
WE(22:1_16:0)	1681799.25	1438236.09	1.17	0.887144456
ChE(38:5)	11793593.01	9583919	1.23	0.887144456
PG(18:2_20:4)	6301020.77	4319869.14	1.46	0.887144456
PE(36:7e)	527141.14	565008.1	0.93	0.969985079
PE(16:1_22:6)	62629348.27	73153444.88	0.86	0.969985079
dMePE(36:7)	62629348.27	73153444.88	0.86	0.969985079
Hex1Cer(d20:1_20:4)	4829663.26	5519227	0.88	0.969985079
PS(20:5_18:2)	2049286.61	2911064.25	0.7	0.969985079
CL(82:11)	21702584.65	25589340.39	0.85	0.969985079
SM(d18:1_24:3)	198290475.5	221630231	0.89	0.969985079
PC(45:2)	307264.63	430622.29	0.71	0.969985079
MGDG(34:1e)	1533407.06	1823557.65	0.84	0.887144456
MGMG(34:1)	1533407.06	1823557.65	0.84	0.887144456

PE, Phosphatidylethanolamine; PC, phosphatidylcholine; TG, triacylglycerol; Cer, Ceramide; BisMePA, Bis(methylthio)phenylacetic acid; WE, Wax Ester; ChE, Cholesteryl Ester; PG, Phosphatidylglycerol; dMePE, Dimethylphosphatidylethanolamine; hex1cer, Hexosylceramide; PS, Phosphatidylserine; CL, Cardiolipin; SM, Sphingomyelin; MGDG, Monogalactosyldiacylglycerol; MGMG, Monogalactosylmonoacylglycerol.

was performed on liver tissues from control, Cd-exposed, and CE+Cd-treated mice (Table 1). Cd exposure resulted in significant perturbations of polyunsaturated fatty acids (PUFA) metabolic pathways compared with controls, reflecting a disruption of hepatic lipid homeostasis. The CE supplementation effectively restored these Cd-induced metabolic alterations. Furthermore, hepatic lipidomic profiling revealed that CE supplementation significantly modulated liver lipid metabolite composition in Cd-exposed mice (Fig. 3a–c, **Supplementary Fig. 1a–d**). Quantitative analysis showed significant reductions in specific phospholipid and TG species in the CE+Cd group relative to Cd-exposed animals, including phosphatidylethanolamine (PE) species (16:1_22:6, 18:0p_22:5, and 36:7e), phosphatidylcholine (PC) derivatives (18:1_14:0, 36:1e, 44:4e, and 45:2), and triacylglycerol (TG) molecules (6:0_14:3_18:2, 11:0_12:2_18:2, and 12:0e_6:0_22:6) (Fig. 3d–k). Transcriptomic analysis revealed significant enrichment of the cytochrome P450 pathway in CE-treated mice compared with Cd-exposed animals (Fig. 3l, **Supplementary Fig. 1e–g**), suggesting a key role of Se in regulating PUFA metabolism. Gene expression profiling demonstrated that Cd exposure significantly upregulated major lipogenic reg-

ulators (*SCD1* and *Ppar γ*) and moderately increased the expression of *Fasn*, *Ppar α* , and *Cpt1 α* , whereas CE treatment effectively reversed these alterations (Fig. 3m–q). Moreover, CE administration significantly reduced Cd-induced elevations of pro-inflammatory cytokines (*Cxcl2* and *Ccl2*) (Fig. 3r,s).

4. Discussion

This study employed the distinctive biomarker levels reported in the Enshi population, serum selenium (416.977 $\mu\text{g/L}$) and urinary cadmium (3.848 $\mu\text{g/L}$), as references for human exposure, allowing reverse calculation of corresponding doses for animal experiments [29, 30]. This approach is consistent with strategies that employ cadmium-based physiologically based pharmacokinetic (PBPK) modeling to establish recommended reference concentrations for diseases such as chronic kidney disease and osteoporosis [31]. Deriving exposure doses from human biomarkers not only demonstrates the feasibility of translating environmental epidemiological data into toxicological studies but also provides a basis for the future development of precise selenium-cadmium combined exposure kinetic models.

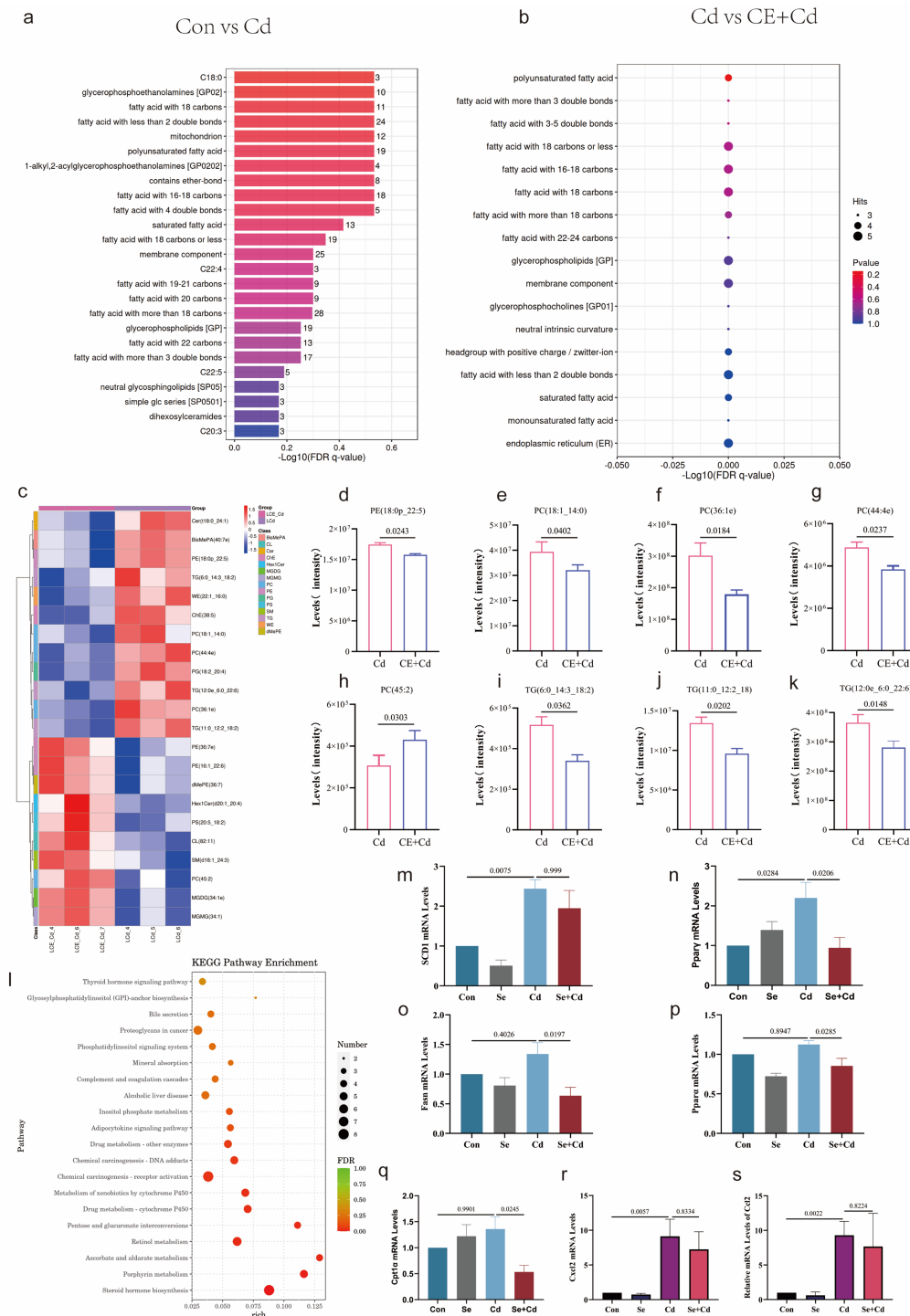


Fig. 3. Se-mediated regulation of lipid metabolism and inflammatory responses in Cd-exposed liver. Lipid functional enrichment analysis of Control vs. Cd (a) and Cd vs. CE+Cd (b) groups. A heatmap shows the relative abundance of significantly altered hepatic lipid metabolites across Control, Cd, and CE+Cd groups, with each row representing a lipid species and each column representing a sample. Z-score normalized intensities are indicated by a color scale from blue (low) to red (high) (c). Quantitative analysis of specific lipid species identified by lipidomics is presented for PE (d–f), PC (g–i), and TG (j,k) in the livers of Control, Cd, and CE+Cd groups. KEGG pathway enrichment analysis based on transcriptomic data from the Cd vs. CE+Cd comparison highlighted significant enrichment of the cytochrome P450 pathway (l). Hepatic mRNA expression levels of key genes involved in lipid metabolism, determined by qRT-PCR, are shown for SCD1 (m), Ppar γ (n), Fasn (o), Ppar α (p), and Cpt1 α (q), with CE treatment suppressing Cd-induced upregulation of lipogenic genes. Hepatic mRNA levels of pro-inflammatory cytokines Cxcl2 (r) and Ccl2 (s) were also significantly reduced by CE administration. Data are presented as mean \pm SEM, (n = 6–10).

Ferroptosis is a novel iron-dependent form of programmed cell death driven by lipid peroxidation [32]. Selenium and its associated selenoproteins are key inhibitors of ferroptosis [33]. Previous study has shown that cadmium can induce ferroptosis through nuclear translocation of the antioxidant transcription factor Nrf2 [34]. In comparison, inhibition of the TXNRD1/Nrf2 pathway, an essential component of mammalian antioxidant defense, *via* agents such as auranofin enhances Nrf2 activation [35]. Our previous work demonstrated that selenium effectively counteracts ferroptosis induced by RSL3 through targeting TXNRD1 [36]. This study further shows that selenium supplementation (CE) exerts anti-ferroptotic effects by regulating PUFA metabolism. Consistent with previous reports indicating that selenium mitigates doxorubicin-induced ferroptosis by reducing key phospholipids involved in lipid peroxidation, such as PE and PC [24], our data reveal that CE treatment significantly restored cadmium-induced PUFA metabolic disturbances, reversing aberrant changes in specific PEs (e.g., 16:1_22:6, 18:0p_22:5) and PC derivatives.

Further analysis indicates that activation of the PPAR γ /SCD1 pathway during the early phase of Cd exposure represents a central mechanism driving further lipid metabolic disorders. Cadmium exposure upregulates PPAR γ and SCD1 expression, resulting in significant PUFA accumulation, consistent with the classical regulatory cascade in which PPAR γ transcriptionally controls SCD1 [37], and SCD1 mediates triglyceride accumulation [38]. We propose that under sustained cadmium stress, the PUFA pool generated by the PPAR γ /SCD1 axis becomes unstable and is readily converted into lipid peroxidation products, including 15-HETE, 4-HNE, and MDA. These oxidized lipid derivatives have been reported to act as endogenous ligands for PPAR γ [39], leading to a self-amplifying cycle of “From PPAR γ activation to PUFA accumulation to lipid peroxidation and back to PPAR γ reactivation” that exacerbates lipid metabolic imbalance. CE treatment effectively suppressed the overactivation of PPAR γ and SCD1, interrupting this cycle. Lipidomic profiling further revealed that cadmium exposure significantly disrupted membrane phospholipid side-chain integrity, an early indicator of hepatocyte injury [40]. SCD1-mediated lipid reprogramming also directly activates inflammatory signaling pathways, such as NF- κ B, promoting chemokine release [41], which explains the observed upregulation of Cxcl2 and Ccl2 in cadmium-exposed livers. By modulating upstream lipid metabolic networks, particularly restoring PUFA homeostasis and inhibiting SCD1, CE not only repaired the membrane lipid environment but also blocked the pathological progression from lipotoxicity to inflammation at its origin.

Different chemical forms of selenium display distinct biological activities [42]. The major selenium species present in the Se-enriched CE used in this study were selenocysteine (SeCys₂) [43]. Organic selenium generally

exhibits higher bioavailability and tissue retention compared to inorganic forms [44] and demonstrates greater efficacy in regulating lipid metabolism-related genes, such as PPAR γ , and in mitigating hepatic steatosis [26]. In this study, both CE and selenomethionine interventions significantly reduced serum TC and TG levels. These results are consistent with previous reports showing that selenium nanoparticles ameliorate metabolic-associated steatohepatitis (MASH) and that sodium selenite improves alcoholic fatty liver disease [26,45], supporting the role of selenium supplementation in counteracting cadmium-induced inflammatory injury through modulation of lipid metabolism.

5. Limitations and Future Directions

Although this study demonstrates selenium’s protective effects against cadmium toxicity *via* regulation of lipid metabolism and inflammatory responses, several limitations remain in the molecular mechanisms and experimental design. First, the intervention period was four weeks. While significant protective effects were observed, this relatively short duration may have limited the evaluation of long-term outcomes under chronic cadmium exposure. Second, as a water extract, CE represents a complex mixture. Although previous studies indicate that its primary active component is organic selenium, and SeMet was included as a control in this study, other coexisting phytochemicals may exert synergistic effects. To clarify selenium’s specific contribution to CE’s protective effects, future studies should incorporate more refined control groups, including purified SeCys₂, selenium-enriched CE, and selenium-depleted CE, to systematically identify the independent and combined actions of each component.

No specific therapeutic agents currently exist for cadmium exposure. Based on the significant antagonistic effects of CE observed here, we plan to implement a human intervention study in cadmium-polluted regions. Participants will receive selenium preparations derived from *Cardamine ensliensis*, with dynamic monitoring of blood selenium metabolites, cadmium body burden, and hepatic and renal function markers. This study aims to validate the “selenium–cadmium antagonism” mechanism in humans and provide evidence-based strategies for health interventions in populations exposed to environmental heavy metals.

6. Conclusions

Se-enriched CE effectively mitigates cadmium-induced hepatotoxicity at environmentally relevant exposure levels. The protective mechanism involves a dual pathway: CE inhibits overactivation of the PPAR γ /SCD1 signalling axis, correcting PUFA metabolic disorders and restoring membrane phospholipid homeostasis in hepatocytes; simultaneously, by remodelling the lipid microenvironment, it suppresses the release of lipid perox-

idation driven inflammatory mediators (Cxcl2, Ccl2) and potential ferroptotic processes. These findings elucidate the molecular basis by which selenium counteracts heavy metal toxicity through a “metabolism immunity” network and provide experimental support for the application of naturally selenium-enriched plant resources in mitigating environmental cadmium exposure at physiologically relevant doses.

Availability of Data and Materials

The data supporting the findings of this study are available from the corresponding author upon reasonable request.

Author Contributions

ZW, XC performed the research study. Data analysis was conducted by ZW and XC. The manuscript was written and revised by ZW, XC, XP, KL, CZ and ZZ contributed to data acquisition, participated in experiments, prepared figures and tables, and performed literature searches. They also participated in revising the manuscript. HW, CH designed the research study, contributed to manuscript revision and funding acquisition. All authors participated in editorial changes and read and approved the final manuscript. All authors have participated sufficiently in the work and agreed to be accountable for all aspects of the work.

Ethics Approval and Consent to Participate

All animal experiments were conducted in accordance with the Regulations for the Administration of Affairs Concerning Experimental Animals of China and relevant institutional guidelines. The experimental protocol was approved by the Animal Ethics Committee of Enshi Tujia and Miao Autonomous Prefecture Central Hospital (Approval No. 202101001).

Acknowledgment

The authors would like to thank all the reviewers who participated in the review and MJEditor for its linguistic assistance during the preparation of this manuscript.

Funding

This work was supported by the Natural Science Foundation of Hubei Province (2025AFD137).

Conflict of Interest

The authors declare no conflict of interest.

Declaration of AI and AI-Assisted Technologies in the Writing Process

During the preparation of this work, the authors used DeepSeek to check spelling and grammar. The scientific content was written entirely independently by the authors, without the use of AI tools. We hope this clarification ad-

dresses the issues raised concerning the use of artificial intelligence in our submitted paper. The authors bear full responsibility for the accuracy, completeness, and scientific rigour of the content presented herein.

Supplementary Material

Supplementary material associated with this article can be found, in the online version, at <https://doi.org/10.31083/FBL50288>.

References

- [1] Satarug S, Garrett SH, Sens MA, Sens DA. Cadmium, environmental exposure, and health outcomes. *Environmental Health Perspectives*. 2010; 118: 182–190. <https://doi.org/10.1289/ehp.0901234>.
- [2] Hoet P, Haufroid V, Deumer G, Dumont X, Lison D, Hantson P. Acute kidney injury following acute liver failure: potential role of systemic cadmium mobilization? *Intensive Care Medicine*. 2012; 38: 467–473. <https://doi.org/10.1007/s00134-011-2449-0>.
- [3] Wang L, Zhang S, Wang Z, Xu M, Yuan L, Cui J, *et al.* A protective role of Heme-regulated eIF2 α kinase in cadmium-induced liver and kidney injuries. *Chemosphere*. 2017; 185: 284–289. <https://doi.org/10.1016/j.chemosphere.2017.07.018>.
- [4] Cengiz M, Gür B, Sezer CV, Cengiz BP, Gür F, Bayraktar A, *et al.* Alternations in interleukin-1 β and nuclear factor kappa beta activity (NF-kB) in rat liver due to the co-exposure of Cadmium and Arsenic: Protective role of curcumin. *Environmental Toxicology and Pharmacology*. 2023; 102: 104218. <https://doi.org/10.1016/j.etap.2023.104218>.
- [5] Gao M, Li C, Xu M, Liu Y, Cong M, Liu S. LncRNA MT1DP Aggravates Cadmium-Induced Oxidative Stress by Repressing the Function of Nrf2 and is Dependent on Interaction with miR-365. *Advanced Science (Weinheim, Baden-Wurttemberg, Germany)*. 2018; 5: 1800087. <https://doi.org/10.1002/advs.201800087>.
- [6] Raeeszadeh M, Moradian M, Khademi N, Amiri AA. The Effectiveness of Time in Treatment with Vitamin C and Broccoli Extract on Cadmium Poisoning in Mice: Histological Changes of Testicular Tissue and Cell Apoptotic Index. *Biological Trace Element Research*. 2024; 202: 3278–3292. <https://doi.org/10.1007/s12011-023-03898-4>.
- [7] Matović V, Buha A, Đukić-Čosić D, Bulat Z. Insight into the oxidative stress induced by lead and/or cadmium in blood, liver and kidneys. *Food and Chemical Toxicology: an International Journal Published for the British Industrial Biological Research Association*. 2015; 78: 130–140. <https://doi.org/10.1016/j.fct.2015.02.011>.
- [8] Andjelkovic M, Buha Djordjevic A, Antonijevic E, Antonijevic B, Stanic M, Kotur-Stevuljevic J, *et al.* Toxic Effect of Acute Cadmium and Lead Exposure in Rat Blood, Liver, and Kidney. *International Journal of Environmental Research and Public Health*. 2019; 16: 274. <https://doi.org/10.3390/ijerph16020274>.
- [9] Ismael MA, Elyamine AM, Moussa MG, Cai M, Zhao X, Hu C. Cadmium in plants: uptake, toxicity, and its interactions with selenium fertilizers. *Metallomics: Integrated Biometal Science*. 2019; 11: 255–277. <https://doi.org/10.1039/c8mt00247a>.
- [10] Luo K, Zhou L, Xie C, Yang Q, Tan L, Lin Q. High-fidelity fluorescent probes for visualizing the inhibitory behavior of selenium on cadmium uptake in rice. *Journal of Hazardous Materials*. 2023; 457: 131748. <https://doi.org/10.1016/j.jhazmat.2023.131748>.
- [11] Hashtjin YA, Raeeszadeh M, Khanghah AP. Interaction of

- Heavy Metals (Cadmium and Selenium) in an Experimental Study on Goldfish: Hematobiochemical Changes and Oxidative Stress. *Journal of Xenobiotics*. 2025; 15: 57. <https://doi.org/10.3390/jox15020057>.
- [12] Cengiz M, Gür B, Sezer CV, Baytar O, Şahin Ö, Ayhancı A, *et al.* Green biosynthesis of selenium and zinc oxide nanoparticles using whole plant extract of *Rheum ribes*: characterization, anticancer, and antimicrobial activity. *Journal of Molecular Liquids*. 2024; 412: 125861. <https://doi.org/10.1016/j.molliq.2024.125861>.
- [13] Huang F, Chen L, Zhou Y, Huang J, Wu F, Hu Q, *et al.* Exogenous selenium promotes cadmium reduction and selenium enrichment in rice: Evidence, mechanisms, and perspectives. *Journal of Hazardous Materials*. 2024; 476: 135043. <https://doi.org/10.1016/j.jhazmat.2024.135043>.
- [14] Chang C, Zhang H, Huang F, Feng X. Understanding the translocation and bioaccumulation of cadmium in the Enshi seleniferous area, China: Possible impact by the interaction of Se and Cd. *Environmental Pollution (Barking, Essex: 1987)*. 2022; 300: 118927. <https://doi.org/10.1016/j.envpol.2022.118927>.
- [15] Li LL, Cui YH, Lu LY, Liu YL, Zhu CJ, Tian LJ, *et al.* Selenium Stimulates Cadmium Detoxification in *Caenorhabditis elegans* through Thiols-Mediated Nanoparticles Formation and Secretion. *Environmental Science & Technology*. 2019; 53: 2344–2352. <https://doi.org/10.1021/acs.est.8b04200>.
- [16] Li C, Xiang Y, Liu M, Wang Z, Wu Y, Yang Q, *et al.* Selenium alleviates cadmium-induced biological aging acceleration and the potential mediating role of inflammation. *Ecotoxicology and Environmental Safety*. 2025; 299: 118361. <https://doi.org/10.1016/j.ecoenv.2025.118361>.
- [17] Wang M, Wang Y, Wang S, Hou L, Cui Z, Li Q, *et al.* Selenium alleviates cadmium-induced oxidative stress, endoplasmic reticulum stress and programmed necrosis in chicken testes. *The Science of the Total Environment*. 2023; 863: 160601. <https://doi.org/10.1016/j.scitotenv.2022.160601>.
- [18] Wang T, Li H, Li Y, Li M, Zhao H, Zhang W, *et al.* Selenomethionine supplementation mitigates fluoride-induced liver apoptosis and inflammatory reactions by blocking Parkin-mediated mitophagy in mice. *The Science of the Total Environment*. 2024; 951: 175458. <https://doi.org/10.1016/j.scitotenv.2024.175458>.
- [19] Ramírez-Acosta S, Uhlířová R, Navarro F, Gómez-Ariza JL, García-Barrera T. Antagonistic Interaction of Selenium and Cadmium in Human Hepatic Cells Through Selenoproteins. *Frontiers in Chemistry*. 2022; 10: 891933. <https://doi.org/10.3389/fchem.2022.891933>.
- [20] Zwolak I. The Role of Selenium in Arsenic and Cadmium Toxicity: an Updated Review of Scientific Literature. *Biological Trace Element Research*. 2020; 193: 44–63. <https://doi.org/10.1007/s12011-019-01691-w>.
- [21] Zhang L, Shi WY, Xu JY, Liu Y, Wang SJ, Zheng JY, *et al.* Protective effects and mechanism of chemical- and plant-based selenocystine against cadmium-induced liver damage. *Journal of Hazardous Materials*. 2024; 468: 133812. <https://doi.org/10.1016/j.jhazmat.2024.133812>.
- [22] Ge J, Liu LL, Cui ZG, Talukder M, Lv MW, Li JY, *et al.* Comparative study on protective effect of different selenium sources against cadmium-induced nephrotoxicity via regulating the transcriptions of selenoproteome. *Ecotoxicology and Environmental Safety*. 2021; 215: 112135. <https://doi.org/10.1016/j.ecoenv.2021.112135>.
- [23] Benvenga S, Marini HR, Micali A, Freni J, Pallio G, Irrera N, *et al.* Protective Effects of Myo-Inositol and Selenium on Cadmium-Induced Thyroid Toxicity in Mice. *Nutrients*. 2020; 12: 1222. <https://doi.org/10.3390/nu12051222>.
- [24] Barchielli G, Capperucci A, Tanini D. The Role of Selenium in Pathologies: An Updated Review. *Antioxidants (Basel, Switzerland)*. 2022; 11: 251. <https://doi.org/10.3390/antiox11020251>.
- [25] Zhang L, Shi WY, Zhang LL, Sha Y, Xu JY, Shen LC, *et al.* Effects of selenium-cadmium co-enriched Cardamine hupingshanensis on bone damage in mice. *Ecotoxicology and Environmental Safety*. 2024; 272: 116101. <https://doi.org/10.1016/j.ecoenv.2024.116101>.
- [26] Zhang Z, Fan B, Zhou C, Zhang P, Liu C, Xiang Y, *et al.* Biomimetic Selenium-Nanocomposites Alleviate MASH by Modulating Lipid and Iron Homeostasis. *Advanced Healthcare Materials*. 2025; 14: e2500467. <https://doi.org/10.1002/adhm.202500467>.
- [27] Long MT, Pedley A, Colantonio LD, Massaro JM, Hoffmann U, Muntner P, *et al.* Development and Validation of the Framingham Steatosis Index to Identify Persons With Hepatic Steatosis. *Clinical Gastroenterology and Hepatology: the Official Clinical Practice Journal of the American Gastroenterological Association*. 2016; 14: 1172–1180.e2. <https://doi.org/10.1016/j.cgh.2016.03.034>.
- [28] Xuan Y, Wu D, Zhang Q, Yu Z, Yu J, Zhou D. Elevated ALT/AST ratio as a marker for NAFLD risk and severity: insights from a cross-sectional analysis in the United States. *Frontiers in Endocrinology*. 2024; 15: 1457598. <https://doi.org/10.3389/fendo.2024.1457598>.
- [29] Li M, Qiu L, Ai X, Xu K, Peng M, Sun G, *et al.* Effects of Selenium and Cadmium on Human Liver and Kidney Functions in Exposed Black Shale Areas. *GeoHealth*. 2024; 8: e2024GH001040. <https://doi.org/10.1029/2024GH001040>.
- [30] Li M, Yang B, Ju Z, Qiu L, Xu K, Wang M, *et al.* Do high soil geochemical backgrounds of selenium and associated heavy metals affect human hepatic and renal health? Evidence from Enshi County, China. *The Science of the Total Environment*. 2023; 883: 163717. <https://doi.org/10.1016/j.scitotenv.2023.163717>.
- [31] Tang Y, Lyu T, Cao H, Zhang W, Zhang R, Liu S, *et al.* Recommendations for the reference concentration of cadmium exposure based on a physiologically based toxicokinetic model integrated with a human respiratory tract model. *Journal of Hazardous Materials*. 2024; 477: 135323. <https://doi.org/10.1016/j.jhazmat.2024.135323>.
- [32] Rochette L, Dogon G, Rigal E, Zeller M, Cottin Y, Vergely C. Lipid Peroxidation and Iron Metabolism: Two Corner Stones in the Homeostasis Control of Ferroptosis. *International Journal of Molecular Sciences*. 2022; 24: 449. <https://doi.org/10.3390/ijms24010449>.
- [33] Sousa JA, Callejas BE, Wang A, Higgins E, Herik A, Andonian N, *et al.* GPx1 deficiency confers increased susceptibility to ferroptosis in macrophages from individuals with active Crohn's disease. *Cell Death & Disease*. 2024; 15: 903. <https://doi.org/10.1038/s41419-024-07289-y>.
- [34] Luo T, Song S, Wang S, Jiang S, Zhou B, Song Q, *et al.* Mechanistic insights into cadmium-induced nephrotoxicity: NRF2-Driven HO-1 activation promotes ferroptosis via iron overload and oxidative stress in vitro. *Free Radical Biology & Medicine*. 2025; 235: 162–175. <https://doi.org/10.1016/j.freeradbiomed.2025.04.047>.
- [35] Sabatier P, Beusch CM, Gencheva R, Cheng Q, Zubarev R, Arnér ESJ. Comprehensive chemical proteomics analyses reveal that the new TRI-1 and TRI-2 compounds are more specific thioredoxin reductase 1 inhibitors than auranofin. *Redox Biology*. 2021; 48: 102184. <https://doi.org/10.1016/j.redox.2021.102184>.
- [36] Cheff DM, Huang C, Scholzen KC, Gencheva R, Ronzetti MH, Cheng Q, *et al.* The ferroptosis inducing compounds RSL3 and ML162 are not direct inhibitors of GPX4 but of TXNRD1. *Redox Biology*. 2023; 62: 102703. <https://doi.org/10.1016/j.redox.2023.102703>.

- [37] Yao D, Luo J, He Q, Shi H, Li J, Wang H, *et al.* SCD1 Alters Long-Chain Fatty Acid (LCFA) Composition and Its Expression Is Directly Regulated by SREBP-1 and PPAR γ 1 in Dairy Goat Mammary Cells. *Journal of Cellular Physiology*. 2017; 232: 635–649. <https://doi.org/10.1002/jcp.25469>.
- [38] Liu HH, Xu Y, Li CJ, Hsu SJ, Lin XH, Zhang R, *et al.* An SCD1-dependent mechanoresponsive pathway promotes HCC invasion and metastasis through lipid metabolic reprogramming. *Molecular Therapy: the Journal of the American Society of Gene Therapy*. 2022; 30: 2554–2567. <https://doi.org/10.1016/j.ymthe.2022.03.015>.
- [39] Abshirini M, Ilesanmi-Oyelere BL, Kruger MC. Potential modulatory mechanisms of action by long-chain polyunsaturated fatty acids on bone cell and chondrocyte metabolism. *Progress in Lipid Research*. 2021; 83: 101113. <https://doi.org/10.1016/j.plipres.2021.101113>.
- [40] Sun B, Ding X, Tan J, Zhang J, Chu X, Zhang S, *et al.* TM6SF2 E167K variant decreases PNPLA3-mediated PUFA transfer to promote hepatic steatosis and injury in MASLD. *Clinical and Molecular Hepatology*. 2024; 30: 863–882. <https://doi.org/10.3350/cmh.2024.0268>.
- [41] Sun Q, Xing X, Wang H, Wan K, Fan R, Liu C, *et al.* SCD1 is the critical signaling hub to mediate metabolic diseases: Mechanism and the development of its inhibitors. *Biomedicine & Pharmacotherapy = Biomedecine & Pharmacotherapie*. 2024; 170: 115586. <https://doi.org/10.1016/j.biopha.2023.115586>.
- [42] Feng R, Wang L, Yang J, Zhao P, Zhu Y, Li Y, *et al.* Underlying mechanisms responsible for restriction of uptake and translocation of heavy metals (metalloids) by selenium via root application in plants. *Journal of Hazardous Materials*. 2021; 402: 123570. <https://doi.org/10.1016/j.jhazmat.2020.123570>.
- [43] Rao S, Yu T, Cong X, Lai X, Xiang J, Cao J, *et al.* Transcriptome, proteome, and metabolome reveal the mechanism of tolerance to selenate toxicity in Cardamine violifolia. *Journal of Hazardous Materials*. 2021; 406: 124283. <https://doi.org/10.1016/j.jhazmat.2020.124283>.
- [44] Ringuet MT, Hunne B, Lenz M, Bravo DM, Furness JB. Analysis of Bioavailability and Induction of Glutathione Peroxidase by Dietary Nanoelemental, Organic and Inorganic Selenium. *Nutrients*. 2021; 13: 1073. <https://doi.org/10.3390/nu13041073>.
- [45] Yang Z, Lian J, Li J, Guo W, Ni L, Lv X. Intestinal Microbiomics and Liver Metabolomics Insights into the Ameliorative Effects of Selenium-Enriched *Lactobacillus fermentum* FZU3103 on Alcohol-Induced Liver Injury in Mice. *Journal of Agricultural and Food Chemistry*. 2025; 73: 3232–3245. <https://doi.org/10.1021/acs.jafc.4c06072>.